ON THE APPLICATION OF HAAR WAVELETS TO LOCALLY PROGRESSIVE ENCODING OF GREY-LEVEL IMAGES

Jonas Valantinas

Department of Applied Mathematics, Kaunas University of Technology
Studentų St. 50-325c, LT-51368 Kaunas, Lithuania

Abstract. In the paper, a new original procedure for the evaluation of discrete Haar spectra for separate fragments (blocks) of a digital image is proposed. The procedure explores specific properties of Haar wavelets, refers to the assumption that Haar spectrum of the whole image is known, and is much faster than direct evaluation of Haar spectral coefficients for the respective image blocks.

It is shown that the developed procedure can be successfully applied to implementing of a locally progressive image encoding idea. The essence of the latter – selected blocks of the image under processing are compressed into a bit stream with increasing accuracy. To translate the idea into action, direct employment of hyperbolic image filters is proposed. Preliminary experimental results show that the developed approach leads to reasonable image compression ratios and sufficiently high quality of restored image blocks..

Keywords: Haar wavelets, digital images, hyperbolic image filtering, image compression.

1. Introduction

The whole set of digital image encoding (compression) techniques can be roughly divided into a pair of groups. The commonly underlined features of image compression algorithms falling into the first group are – reduction of the number of grey levels in the image under processing (Block – Truncation – Coding algorithms, [1]), detection of block similarities within the image (finite automata based compression methods, [2, 3], fractal image encoding procedures, [4, 5, 6]), preliminary change of image dimensionality, [7], and so forth. All the enumerated techniques are efficient enough – image compression ratios vary from 5 to 25, ensuring acceptable quality of restored images. Nevertheless, throughout the last two short decades, for certain increased attention was paid to fractal image compression technologies. Despite the intractable asymmetry problem (prolonged image encoding time and fast decoding), the fractal approach till now is considered to be very attractive, perspective and cherishing a hope, especially at high image compression ratios, [8, 9, 10].

The distinguishing feature of image compression algorithms falling into the second group - initial data (arrays of pixel values) are preliminary transformed into the spectral domain by means of a particular discrete transform (Walsh-Hadamard, cosine, wavelet, etc., [11]), i.e. not the image itself but its discrete spectrum is analyzed and processed. The compression effect, in many cases, is achieved by ignoring high-frequency components of the image. Among the "members" of the group there are – the still image compression standard JPEG, [12, 13], hyperbolic image filters, [14, 15], wavelet-based image encoding techniques, [16, 17], and others. In the past ten years, special attention was paid to wavelet-based progressive (embedded) image compression technologies, [18, 19, 20]. The discrete wavelet spectrum of an image is compressed into a bit stream with increasing accuracy. This means that when more bits are added to the stream, the restored image will contain more detail, a property similar to JPEG – 2000 encoded images, [13].

In this paper, a new locally progressive image encoding strategy (approach) is proposed. Increased accuracy is addressed not to the whole restored image but to separate selected blocks of the image. Specific properties of Haar wavelets, as well as a newly developed original procedure for finding of Haar spectral coefficients for image blocks, ensure sufficiently high overall performance of the approach.

2. Haar wavelets and their properties

An orthogonal system of Haar functions (wavelets) is usually introduced using expressions:
$haar(0, 0, x) = 1$, $x \in [0,1)$;

$$haar(r,m,x) = \begin{cases} \sqrt{2^r}, & (m-1)/2^r \le x < (m-1/2)/2^r \\ -\sqrt{2^r}, & (m-1/2)/2^r \le x < m/2^r \\ 0, & \text{otherwise,} \end{cases}$$

where: $r = 0, 1, 2, ...$; $m = 1, 2, ..., 2^r$ (Figure 1).

Haar (wavelet) expansions have a number of good properties not available in other types of expansions (Fourier, Walsh, etc.). To see this in the simplest context, consider a one-dimensional analogue image (signal) $f(x)$ on the interval $[0, 1]$. We can expand it in a Haar function series

$$f(x) = c_0 + \sum_{r=0}^{\infty} \sum_{m=1}^{2^r} c_{rm} \cdot \Psi(2^r x - m + 1), \qquad (1)$$

where: c_0, c_{rm} $(r = 0, 1, 2...; m = 1, 2, ..., 2^r)$ are Haar coefficients; $\Psi(x) = 1$, for $0 \le x < 1/2$, $\Psi(x) = -1$, for $1/2 \le x < 1$, and $\Psi(x) = 0$, otherwise; also, let us observe here that

$$\Psi(2^r x - m + 1) = 1/\sqrt{2^r} \cdot haar(r, m, x),$$

for all values of r and m; $x \in [0,1)$.

Haar series (equation (1)) is very well localized in space (the distinguishing property of wavelets!) – if one is interested in the behaviour of $f(x)$ on a subinterval $[a, b] \subset [0, 1)$ one needs only to take the sum (in (1)) over those indices for which the interval $I_{rm} = [2^{-r}(m-1); 2^{-r}m]$ (the support of the Haar wavelet $\Psi(2^r x - m + 1)$) intersects $[a, b]$. Furthermore, the partial sum of the Haar series (summing $0 \le r \le N$) represents an approximation to $f(x)$ taking into account details on the order of magnitude 2^{-N} or greater.
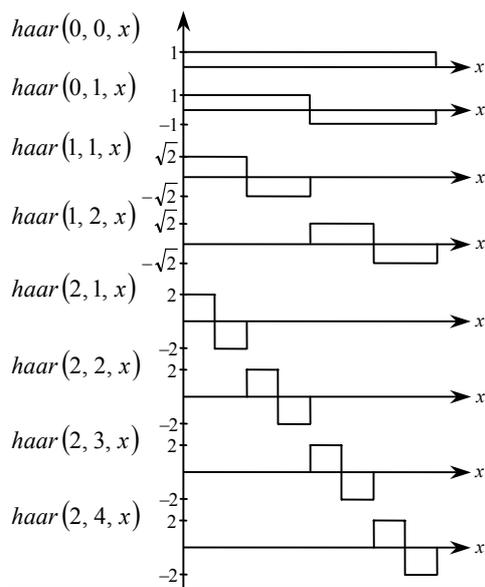
Figure 1. Haar wavelets ($N = 8$)

As it can be seen, Haar wavelets are created out of a single function ("mother" wavelet) $\Psi(x)$ by dyadic dilations and integer translations (expression (1)). Evidently, localization in space and the latter property (scaling) are the hallmarks of Haar (wavelet) expansions.

Due to these properties, Haar wavelets (Haar expansions, discrete Haar representations) find various interesting applications in the digital image (signal) processing area.

Below, we present developments on the application of Haar wavelets to locally progressive encoding of digital grey-level images.

2.1. The discrete Haar transform

Consider a one-dimensional digital image $X = [X(m)] = (X(0)\,X(1)...\,X(N-1))^T$, $N = 2^n, n \in N$, $X(m) \in \{0, 1, ..., 2^p - 1\}$, for all $m = 0, 1, ..., N-1$; here p ($p > 1$) stands for the number of bits attached to encode pixel values in the image.

The discrete Haar (wavelet) transform (HT) for the image X is defined to be:

$$Y = [Y(k)] = \frac{1}{N} H(n) \cdot X;$$

here $H(n)$ is an orthogonal HT matrix of order n, obtained by discretizing a finite number of Haar functions (Figure 1). The vector

$$Y = [Y(k)] = (Y(0)\,Y(1)...\,Y(N-1))^T$$

is said to be the HT spectrum of the image X.

Each spectral coefficient $Y(k)$ $(k \in \{1, 2, ..., N-1\}$ possesses very interesting and valuable (from the practical point of view) properties:

1. The coefficient $Y(k)$ ($k = 2^{n-s} + l$; $s \in \{1, 2, ..., n\}$; $l \in \{0, 1, ..., 2^{n-s} - 1\}$) is associated with an image fragment (block) $X_k = [X_k(m)]$, where $m \in V_k = \{l \cdot 2^s, l \cdot 2^s + 1, ..., (l+1) \cdot 2^s - 1\}$, i.e., this and only this image block specifies numerical value of $Y(k)$; besides, parameter s stands for the scale level (low scale means high resolution).

2. A subset (tree) of spectral coefficients can be attached to $Y(k)$ (provided $s > 1$), namely:

$$\{Y(k^*) \mid k^* \in \mathfrak{I}_k = \bigcup_{t=1}^{s-1} \{2^t k, 2^t k + 1, ..., 2^t (k+1) - 1\}\}.$$

Worth emphasizing that all spectral coefficients (vertices of the tree) $Y(k^*)$, $k^* \in \mathfrak{I}_k$, are associated with the same image block X_k (more precisely, with subsets of X_k). Often, the spectral coefficient $Y(k)$ is called the root of the tree (Figure 2).

178

The above-enumerated properties can be generalized to include two-dimensional digital images. Suppose, $[X(m_1, m_2)]$ and $[Y(k_1, k_2)]$ $(m_1, m_2, k_1, k_2 \in \{0, 1, ..., N-1\}$; $N = 2^n$, $n \in \mathbb{N})$ stand for the two-dimensional grey-level image and its discrete Haar spectrum, respectively.

Consider the spectral coefficient $Y(k_1, k_2)$, $(k_1, k_2) \notin \{(0, 0), (0,1), (1, 0), (1, 1)\}$. In regard to $Y(k_1, k_2)$ we can state the following:

1. The coefficient $Y(k_1, k_2)$ $(k_r = 2^{n-s_r} + l_r;$ $l_r \in \{0, 1, ..., 2^{n-s_r} - 1\}$, $r = 1, 2$) is associated with an image block

$$X_{k_1, k_2} = [X(m_1, m_2) \,|\, (m_1, m_2) \in V_{k_1} \times V_{k_2}],$$

where $V_{k_r} = \{l_r \cdot 2^{s_r}, \ l_r \cdot 2^{s_r} + 1, ..., (l_r + 1) \cdot 2^{s_r} - 1\}$, $r=1, 2$. In other words, numerical value of $Y(k_1, k_2)$ is defined exceptionally by X_{k_1, k_2} (localization in space!).

2. A subset of spectral coefficients (quad-tree) can be attached to $Y(k_1, k_2)$, provided $s_1 > 1$ and $s_2 > 1$. The vertices (spectral coefficients) of the quad-tree are given by

$$\{Y(k_1^*, k_2^*) \,|\, (k_1^*, k_2^*) \in \bigcup_{t=1}^{\min\{s_1-1, s_2-1\}} (\Im_{k_1}(t) \times \Im_{k_2}(t))\},$$

$\Im_{k_r}(t) = \{2^t \cdot k_r, \ 2^t \cdot k_r + 1, ..., 2^t(k_r + 1) - 1\}$, for all $t = 1, 2, ..., s_r - 1; \quad r = 1, 2$.

In Figure 3, a graphical interpretation of enumerated properties, attached to Haar spectral coefficients of the two-dimensional digital image, is presented.
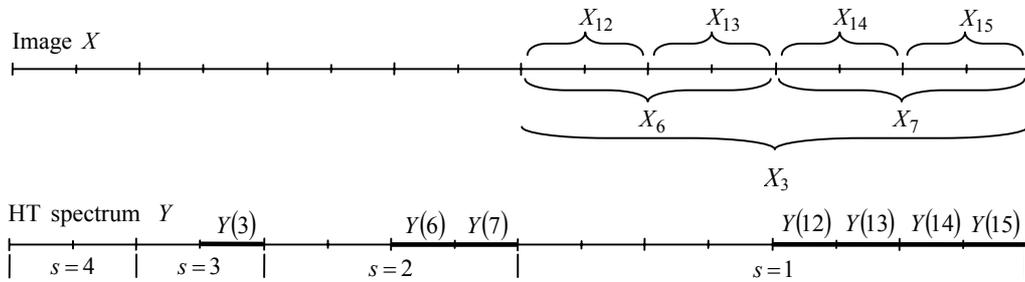
Figure 2. Graphical interpretation of properties of Haar spectral coefficients ($\Im_3 = \{6, 7, 12, 13, 14, 15\}$ represents the tree, attached to the spectral coefficient (root of the tree) $Y(3)$; $N = 16$)
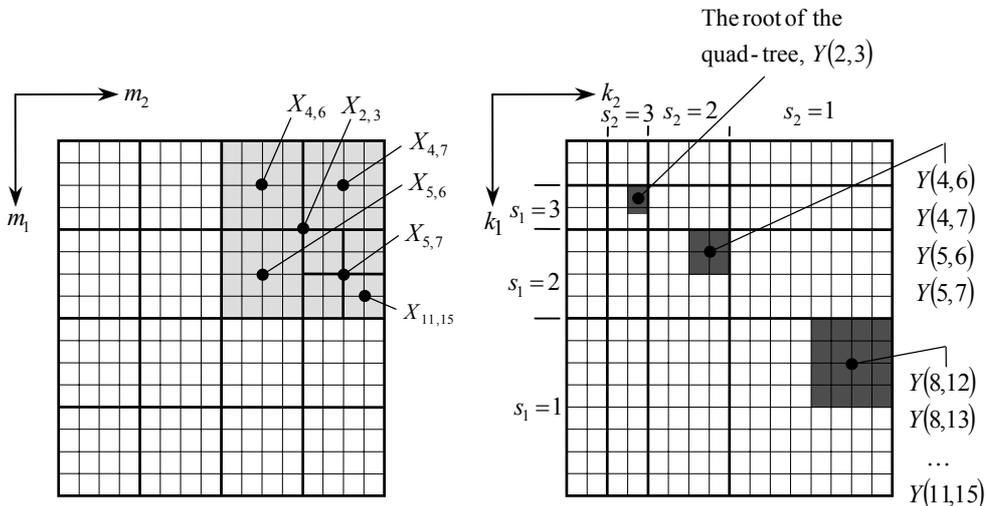
Figure 3. Graphical interpretation of properties of Haar spectral coefficients: (a) image $[X(m_1, m_2)]$, $N = 16$; the coefficient $Y(2, 3)$ is associated with the image block $X_{2,3}$; (b) the quad-tree, attached to the Haar coefficient $Y(2, 3)$ ($\Im_2 = \{4, 5, 8, 9, 10, 11\}$, $\Im_3 = \{6, 7, 12, 13, 14, 15\}$)

The two mentioned properties (localization in space and availability of quad-trees in HT spectrum of the image) made it possible to describe, to develop and to put into action a very interesting and perspective grey-level image encoding idea – EZW (Embedded – Zero-tree – Wavelet) coding algorithm, [16].

In the sections below, we propose a novel modification (approach) – locally progressive encoding of

grey-level images. The essence of the approach – additional bits of information are used to improve quality not of the whole (restored) image but that of selected smaller blocks of the image. Implementation of the idea rests on the fact that HT spectra for selected image blocks can be efficiently found using HT spectrum of the whole image.

2.2. A new approach to the determination of HT spectra for image blocks

Suppose, $X = (X(0)\,X(1)\,...\,X(N-1))^T$ and $Y = (Y(0)\,Y(1)\,...\,Y(N-1))^T$ are a one-dimensional grey-level image and its discrete Haar (wavelet) spectrum, respectively.

Consider the spectral coefficient $Y(k)$ ($k = 2^{n-s} + l$ ($l \in \{2, 3, ..., N-1\}$)), associated with the image fragment (block) $X_k = [X_k(m)]$, $m = l \cdot 2^s$, $l \cdot 2^s + 1$, ..., $(l+1) \cdot 2^s - 1$.

Let us denote the HT spectrum of X_k by

$$Y^{(k)} = (Y^{(k)}(0)\,Y^{(k)}(1)\,...\,Y^{(k)}(2^s-1))^T$$

In the light of properties of Haar wavelets, we have developed a new efficient procedure for the determination of numerical values of $Y^{(k)}(i)$ ($i \in \{0, 1, ..., 2^s - 1\}$), namely: $Y^{(k)}(0) = \overline{X}_k$, $Y^{(k)}(i) = \sqrt{2^{n-s}} \cdot Y(k^*)$, for all $i = 1, 2, ..., 2^s - 1$;

$$k^* \in \{k\}\bigcup \mathfrak{I}_k \ (\mathfrak{I}_k = \bigcup_{t=1}^{s-1}\{2^t k, 2^t k + 1, ..., 2^t(k+1)-1\})$$

and a one-to-one correspondence between the sets $\{1, 2, ..., 2^s - 1\}$ and $\{k\}\bigcup \mathfrak{I}_k$ is fixed; $\overline{X}_k$ signifies the constant component of the image block X_k and is found using recurrent relationships:

$$\overline{X}_k = \overline{X}_{k^\circ} + (-1)^k \sqrt{2^{n-s-1}} \cdot Y(k^\circ);$$

$\overline{X}_0 = \overline{X}_1 = Y(0)$; $k^\circ = [k/2]$, where $[x]$ stands for the integral part of the number x.

For instance, let

$$X = (10\ 20\ 3\ 4\ 5\ 6\ 7\ 8\ 10\ 20\ 3\ 4\ 5\ 6\ 7\ 8)^T$$

be a one-dimensional image. Its discrete HT spectrum

$$Y = (7.875\ \ 0\ \ 0.6875\sqrt{2}\ \ 0.6875\sqrt{2}\ \ 2.875\ \ -0.5$$
$$2.875\ \ -0.5\ \ -1.25\sqrt{2}\ \ -0.125\sqrt{2}\ \ -0.125\sqrt{2}$$
$$-0.125\sqrt{2}\ \ -1.25\sqrt{2}\ \ -0.125\sqrt{2}\ \ -0.125\sqrt{2}$$
$$-0.125\sqrt{2})^T.$$

Consider the spectral coefficient $Y(3)$ associated with the image block $X_3 = (X(8)\,X(9)\,...\,X(15))^T = (10\ 20\ 3\ 4\ 5\ 6\ 7\ 8)^T$. Applying the above relation-

ships (procedure), we easily obtain the HT spectrum $Y^{(3)} = (Y^{(3)}(0)\,Y^{(3)}(1)\,...\,Y^{(3)}(7))^T$ for X_3 (keep in mind, $k = 3 = 2^{4-3} + 1$, i.e., $s = 3$, $l = 1$ and $\mathfrak{I}_3 = \{6, 7, 12, 13, 14, 15\}$):

$$Y^{(3)}(0) = \overline{X}_3 = \overline{X}_1 - \sqrt{2^{4-4}} \cdot Y(1) =$$
$$= Y(0) - Y(1) = 7.875,$$
$$Y^{(3)}(1) = \sqrt{2^{4-3}} \cdot Y(3) = 1.375,$$
$$Y^{(3)}(2) = \sqrt{2} \cdot Y(6) = 2.875\sqrt{2},$$
$$Y^{(3)}(3) = \sqrt{2} \cdot Y(7) = -0.5\sqrt{2},$$
$$Y^{(3)}(4) = \sqrt{2} \cdot Y(12) = -2.5,$$
$$Y^{(3)}(5) = \sqrt{2} \cdot Y(13) = -0.25,$$
$$Y^{(3)}(6) = \sqrt{2} \cdot Y(14) = -0.25,$$
$$Y^{(3)}(7) = \sqrt{2} \cdot Y(15) = -0.25.$$

Thus, the discrete HT spectrum of X_3 is found –
$$Y^{(3)} = (7.875\ \ 1.375\ \ 2.875\sqrt{2}\ \ -0.5\sqrt{2}\ \ -2.5\ \ -0.25$$
$$-0.25\ \ -0.25)^T.$$

Similarly, $Y(6)$ is associated with the image block $X_6 = (X(8)\,X(9)\,X(10)\,X(11))^T = (10\ 20\ 3\ 4)^T$.

Since $k = 6 = 2^2 + 2$ (i.e., $s = 2$, $l = 2$ and $\mathfrak{I}_6 = \{12, 13\}$), we easily compute the HT spectrum $Y^{(6)}$ for X_6:

$$Y^{(6)}(0) = \overline{X}_6 = \overline{X}_3 + \sqrt{2^{4-3}} \cdot Y(3) =$$
$$= \overline{X}_1 - \sqrt{2^{4-4}} \cdot Y(1) + \sqrt{2} \cdot Y(3) =$$
$$= Y(0) - Y(1) + \sqrt{2} \cdot Y(3) = 9.25,$$
$$Y^{(6)}(1) = \sqrt{2^{4-2}} \cdot Y(6) = 5.75,$$
$$Y^{(6)}(2) = 2 \cdot Y(12) = -2.5\sqrt{2},$$
$$Y^{(6)}(3) = 2 \cdot Y(13) = -0.25\sqrt{2}.$$

So, $Y^{(6)} = (9.25\ \ 5.75\ \ -2.5\sqrt{2}\ \ -0.25\sqrt{2})^T$.

A simple analysis of the above relationships, as well as knowledge of the detailed scheme for the direct evaluation of HT spectra for image blocks, made it possible to estimate time expenditures associated with both approaches (direct evaluation, proposed procedure). Comparative analysis was done for one-dimensional image blocks of size 2^s ($5 \leq s \leq n-1$; here 2^n is the size of the whole image X). It was found out that the number of operations (addition, multiplication) needed for direct evaluation of the HT spectrum of the image block X_k, associated with the spectral coefficient $Y(k)$ ($k = 2^{n-s} + l$, $s \in \{5, 6, ..., n-1\}$, $l \in \{0, 1, ..., 2^{n-s} - 1\}$), equaled

$$\mathfrak{R}_d = 2^s + \sum_{t=0}^{s-1} 2^{s-t}(s-t),$$

whereas the newly developed approach (procedure) required

$$\Re_{pr} = 2^s + 2(n-s) - 1$$

operations. The speed gain ρ ($\rho = \Re_d / \Re_{pr}$) is obvious (Table 1).

Table 1. Comparison of two approaches to finding of HT spectra for one-dimensional image blocks of size 2^s ($N = 2^n = 1024$)

s	5	6	7	8	9
$\Re_d$	290	706	1666	3842	8706
$\Re_{pr}$	41	71	133	259	513
ρ	7.07	9.94	12.53	14.83	16.97

Now, consider a two-dimensional grey-level image $[X(m_1, m_2]$ ($m_1, m_2 \in \{0,1,...,N-1\}$). Let $[Y(k_1, k_2]$ be its two-dimensional discrete HT spectrum. Let us designate the discrete HT spectrum of the image block X_{k_1,k_2}, associated with the spectral coefficient $Y(k_1, k_2)$ ($k_r = 2^{n-s_r} + l_r$; $r = 1, 2$) as $Y^{(k_1,k_2)} = [Y^{(k_1,k_2)}(i, j)]$, where $i = 1, 2, ..., 2^{s_1} - 1\}$ and $j = 1, 2, ..., 2^{s_2} - 1\}$.

We have proved that:

1. The spectral coefficient $Y^{(k_1,k_2)}(0,0)$, which coincides with the constant component $\overline{X}_{k_1,k_2}$ of X_{k_1,k_2}, i.e., $Y^{(k_1,k_2)}(0,0) = \overline{X}_{k_1,k_2}$, can be found using recurrent relationships, namely:

$$\overline{X}_{k_1,k_2} = \overline{X}_{k_1^\circ, k_2^\circ} + (-1)^{k_1} \sqrt{2^{n-s_1-1}} \cdot A(k_1^\circ, k_2^\circ) +$$
$$+ (-1)^{k_2} \sqrt{2^{n-s_2-1}} \cdot B(k_1^\circ, k_2^\circ) +$$
$$+ (-1)^{k_1+k_2} \sqrt{2^{2n-s_1-s_2-2}} \cdot Y(k_1^\circ, k_2^\circ),$$
$$\overline{X}_{k_1,0} = \overline{X}_{k_1,1} = \overline{X}_{k_1^\circ, 0} + (-1)^{k_1} \sqrt{2^{n-s_1-1}} \cdot A(k_1^\circ, 0),$$
$$\overline{X}_{0,k_2} = \overline{X}_{1,k_2} = \overline{X}_{0,k_2^\circ} + (-1)^{k_2} \sqrt{2^{n-s_2-1}} \cdot B(0, k_2^\circ),$$

for $k_1 > 1$, $k_2 > 1$; $k_r^\circ = [k_r/2]$, $r = 1, 2$; also,

$$A(k_1, k_2) = \begin{cases} Y(k_1, 0), & k_2 \le 1 \ (s_2 = n) \\ Y(k_1, 0) + \sum_{r=1}^{n-s_2} (-1)^{l_2^{(r)}} \sqrt{2^{n-s_2-r}} \cdot Y(k_1, j_r), \\ \qquad\qquad k_2 > 1 \ (s_2 < n), \end{cases}$$

$$B(k_1, k_2) = \begin{cases} Y(0, k_2), & k_1 \le 1 \ (s_1 = n) \\ Y(0, k_2) + \sum_{r=1}^{n-s_1} (-1)^{l_1^{(r)}} \sqrt{2^{n-s_1-r}} \cdot Y(i_r, k_2), \\ \qquad\qquad k_1 > 1 \ (s_1 < n); \end{cases}$$

here: $i_r = i_{r-1}^\circ$ ($r = 2, 3, ..., n-s_1$), $i_1 = k_1^\circ$; $j_r = j_{r-1}^\circ$ ($r = 2, 3, ..., n-s_2$), $j_1 = k_2^\circ$; $< l_1^{(n-s_1)} l_1^{(n-s_1-1)} ... l_1^{(1)} >$ and

$< l_2^{(n-s_2)} l_2^{(n-s_2-1)} ... l_2^{(1)} >$ are binary representations of the decimal numbers l_1 and l_2, respectively. (Note: $\overline{X}_{0,0} = \overline{X}_{0,1} = \overline{X}_{1,0} = \overline{X}_{1,1} = Y(0,0)$).

2. The spectral coefficients $Y^{(k_1,k_2)}(i, j)$ ($i^2 + j^2 \neq 0$) can be found as follows:

$$Y^{(k_1,k_2)}(i, 0) = \sqrt{2^{n-s_1}} \cdot A(k_1^*, k_2),$$
$$Y^{(k_1,k_2)}(0, j) = \sqrt{2^{n-s_2}} \cdot B(k_1, k_2^*),$$
$$Y^{(k_1,k_2)}(i, j) = \sqrt{2^{2n-s_1-s_2}} \cdot Y(k_1^*, k_2^*),$$

for all $i = 1, 2, ..., 2^{s_1} - 1$ and $j = 1, 2, ..., 2^{s_2} - 1$; here $k_1^* \in \{k_1\} \cup \Im_{k_1}$, $k_2^* \in \{k_2\} \cup \Im_{k_2}$. As before, there is a one-to-one correspondence between the sets $\{1, 2, ..., 2^{s_1} - 1\}$ and $\{k_1\} \cup \Im_{k_1}$ (also, between $\{1, 2, ..., 2^{s_2} - 1\}$ and $\{k_2\} \cup \Im_{k_2}$).

For instance, let us derive expressions for finding HT spectral coefficients of the image block $X_{3,6}$, associated with the spectral coefficient $Y(3,6)$ (suppose the image X itself has dimensions 16x16). Since $k_1 = 3 = 2^{4-3} + 1$ (i.e., $s_1 = 3$, $l_1 = 1$, $\Im_3 = \{6, 7, 12, 13, 14, 15\}$) and $k_2 = 6 = 2^{4-2} + 2$ (i.e., $s_2 = 2$, $l_2 = 2$, $\Im_6 = \{12, 13\}$), we have:

$$Y^{(3,6)}(0,0) = \overline{X}_{3,6} = \overline{X}_{1,3} + (-1)^3 \sqrt{2^{4-3-1}} \cdot A(1, 3) +$$
$$+ (-1)^6 \sqrt{2^{4-2-1}} \cdot B(1, 3) + (-1)^{3+6} \sqrt{2^{8-3-2-2}} \cdot Y(1, 3) =$$
$$= \overline{X}_{0,1} + (-1)^3 \sqrt{2^{4-3-1}} \cdot B(0, 1) - A(1, 3) + \sqrt{2} \cdot B(1, 3) -$$
$$- \sqrt{2} \cdot Y(1, 3) = Y(0, 0) - Y(0, 1) - Y(1, 0) + Y(1, 1) +$$
$$+ \sqrt{2} \cdot Y(0, 3) - \sqrt{2} \cdot Y(1, 3),$$

$$Y^{(3,6)}(1,0) = \sqrt{2^{4-3}} \cdot A(3, 6) = \sqrt{2}(Y(3, 0) - \sqrt{2^{4-2-2}} \cdot Y(3, 1)) = \sqrt{2} \cdot Y(3, 0) + 2Y(3, 3) - \sqrt{2} \cdot Y(3, 1),$$

$$Y^{(3,6)}(2,0) = \sqrt{2} \cdot Y(6, 0) + 2Y(6, 3) - \sqrt{2} \cdot Y(6, 1),$$

$$Y^{(3,6)}(3,0) = \sqrt{2} \cdot Y(7, 0) + 2Y(7, 3) - \sqrt{2} \cdot Y(7, 1),$$

$$Y^{(3,6)}(4,0) = \sqrt{2} \cdot Y(12, 0) + 2Y(12, 3) - \sqrt{2} \cdot Y(12, 1),$$

$$Y^{(3,6)}(5,0) = \sqrt{2} \cdot Y(13, 0) + 2Y(13, 3) - \sqrt{2} \cdot Y(13, 1),$$

$$Y^{(3,6)}(6,0) = \sqrt{2} \cdot Y(14, 0) + 2Y(14, 3) - \sqrt{2} \cdot Y(14, 1),$$

$$Y^{(3,6)}(7,0) = \sqrt{2} \cdot Y(15, 0) + 2Y(15, 3) - \sqrt{2} \cdot Y(15, 1),$$

$$Y^{(3,6)}(0,1) = \sqrt{2^{4-2}} \cdot B(3, 6) = 2(Y(0, 6) - \sqrt{2^{4-3-1}} \cdot Y(1, 6)) = 2Y(0, 6) - 2Y(1, 6),$$

$$Y^{(3,6)}(0,2) = 2Y(0, 12) - 2Y(1, 12),$$

$$Y^{(3,6)}(0,3) = 2Y(0, 13) - 2Y(1, 13),$$

$$Y^{(3,6)}(i,j) = \sqrt{2^{8-3-2}} \cdot Y(k_1^*, k_2^*) = 2\sqrt{2} \cdot Y(k_1^*, k_2^*),$$

for all $i = 1, 2, ..., 7$ and $j = 1, 2, 3$; here $k_1^* \in \{3\} \cup \mathfrak{I}_3$ and $k_2^* \in \{6\} \cup \mathfrak{I}_6$.

We here emphasize that the number of operations (addition, multiplication) needed for direct evaluation of the discrete HT spectrum of the image block X_{k_1, k_2}, associated with the spectral coefficient $Y(k_1, k_2)$ ($k_r = 2^{n-s_r} + l_r$, $r = 1, 2$; $s^1 = s^2 = s \in \{5, 6, ..., n-1\}$; $2^n \times 2^n$ are dimensions of the whole image $[X(m_1, m_2)]$), equals

$$\mathfrak{R}_d = 2^{s+1} \left(2^s + \sum_{t=0}^{s} 2^{s-t}(s-t) \right),$$

whereas the proposed approach (procedure) requires

$$\mathfrak{R}_{pr} = (2^s - 1)^2 + 4(n-s)(2^s - 1) + 10(n-s) - 4$$

operations. The speed gain, expressed in terms of $\rho = \mathfrak{R}_d / \mathfrak{R}_{pr}$, is presented in Table 2.

Table 2. Comparison of two approaches to finding of HT spectra for image blocks of size $2^s \times 2^s$ ($N = 512$)

s	6	7	8
$\mathfrak{R}_d$	90368	426496	1967104
$\mathfrak{R}_{pr}$	4751	17161	66051
ρ	19.02	24.85	29.78

In the context of locally progressive image encoding, the above results (achievable HT spectrum evaluation speed gains) are highly valuable.

3. Locally progressive encoding of grey-level images

In what follows, we shortly present a locally progressive grey-level image encoding idea. Implementation of the idea rests on the direct use of both the hyperbolic image filters and the developed fast procedure for finding HT spectra of selected image blocks.

3.1. The general scheme

The general scheme reflecting implementation of the locally progressive image encoding idea (two-dimensional case) is presented in Figure 3.

It should be emphasized that the locally progressive image encoding idea is kept alive due to the following circumstances:

1. An image fragment (block) under processing is associated (in some sense) with the whole image as a context, i.e., beyond the context the image block is less meaningful.

2. Particular blocks of the image are characterized as being very informative and require to be restored in a greater detail.

The overall high performance of the proposed locally progressive image encoding procedure is attained, mainly, owing to sufficiently high compression ratios of the whole image and comparatively low compression ratios of the selected image blocks.

Since, customarily, the progressive image encoding idea (approach) is realized in a spectral domain, fast passage from the discrete Haar (wavelet) spectrum of the whole image to discrete Haar spectra of the selected image blocks is extremely valuable (plays a key role).

Below, we present implementation of the developed progressive image encoding approach using two-dimensional Haar hyperbolic image filters (Figure 4).

3.2. Implementation of the idea

Hyperbolic image filters can be attached to the class of unsophisticated lossy image encoding techniques.

The hyperbolic image filtering (encoding) idea originally was described by prof. P. Zinterhof (Salzburg University, Austria, 1993) and was referred to process two-dimensional grey-level images, [14]. The idea itself is rather simple.

Consider a two-dimensional grey-level image $[X(m_1, m_2)]$ ($m_1, m_2 \in \{0, 1, ..., N-1\}$). Let $[Y(k_1, k_2)]$ be its two-dimensional discrete HT spectrum. If, now, M is some a priori chosen integer $(1 \le M < (N-1)^2)$, then for storing (transmitting) one must take only those spectral coefficients $Y(k_1, k_2)$, whose serial numbers (k_1, k_2) satisfy the condition $\bar{k}_1 \cdot \bar{k}_2 \le M$ ($\bar{k}_r = \max\{k_r, 1\}$, $r = 1, 2$). When reconstructing the initial image (obtaining its estimate), the rest spectral coefficients ($\bar{k}_1 \cdot \bar{k}_2 > M$) are equated to zero, i.e., high frequency components of the image, at the decompression stage, are ignored (compression effect!). Thus, the hyperbolic filtering idea leans upon the supposition that the human eye is less sensitive to changes in high frequencies than in lower ones.

The characteristic feature of the hyperbolic image filters – their simplicity, easy realization, tolerable image compression ratios.

For practical applications one can make use of the relationships established between the level M of a hyperbolic filter and the corresponding compression ratio β of the grey-level image (or image block) under processing, namely: $\beta = N^2 / f(N, M)$, where

$$f(N, M) = 2\min\{N, M+1\} +$$
$$+ \sum_{k=2}^{\min\{N-1, M\}} \min\left\{N, \left[\frac{M}{k}\right] + 1\right\}$$

represents the total number of stored Haar spectral coefficients of the image (Table 3).

The role of hyperbolic image filters, used to implement the locally progressive image encoding idea, is two-fold: firstly, they are used to compress "heavily" ($\beta_1 \geq 20$) the whole image and, secondly, to compress "softly" ($\beta_2 \leq 5$) the selected image block.
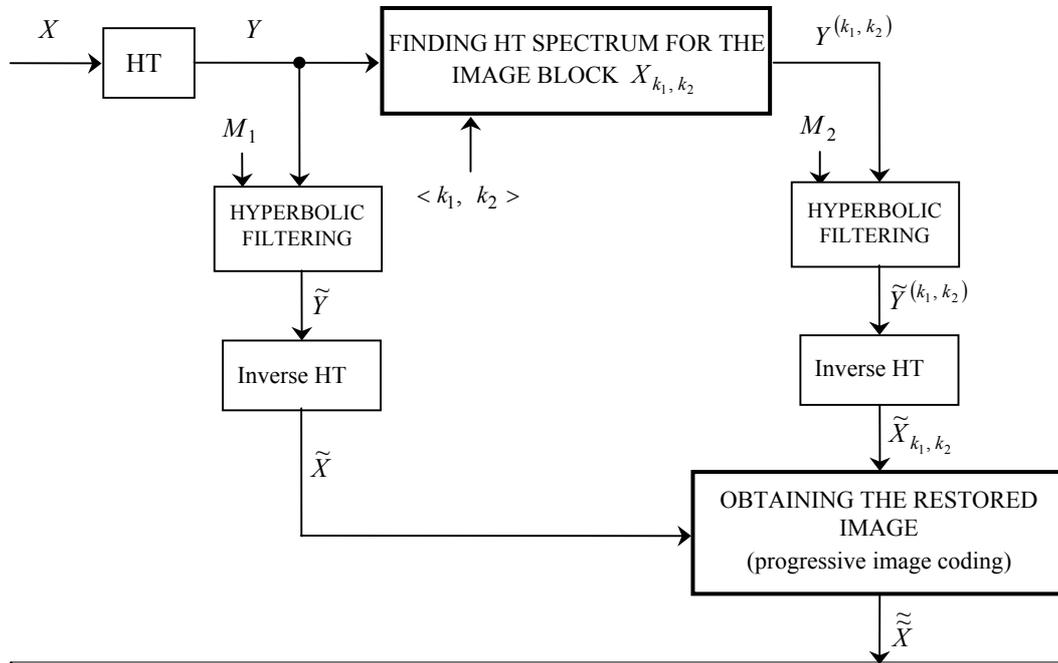
Figure 4. The locally progressive encoding of two-dimensional grey-level images (with the use of hyperbolic image filters)

One can easily ascertain that the overall averaged image compression ratio β equals

$$\beta = \frac{\beta_1 \tau}{\beta_1 + \tau},$$

where: β_1 – compression ratio of the whole image $[X(m_1, m_2]$ with dimensions $2^n \times 2^n$, β_2 – compression ratio of the selected image block with dimensions $2^s \times 2^s$ ($6 \leq s \leq n-1$) and $\tau = \beta_2 \cdot 4^{n-s}$ (Table 4).

Table 3. Relationships between the level M of a hyperbolic image filter and the respective image compression ratio β

β	Image size, $N \times N$			
	512x512	256×256	128×128	64×64
2	48687	12102	2999	734
3	26366	6544	1611	389
4	17569	4349	1064	254
5	12959	3199	779	183
10	5235	1273	303	65
15	3123	749	175	45
20	2175	512	118	35
25	1642	389	96	29
30	1308	299	83	24
40	908	216	64	19

In a particular case (for images of size 512×512; Table 4) we have – the overall image compression ratio $\beta > 24$, provided $\beta_1 \geq 30$ and $\beta_2 = 2$ (for image blocks of size 64x64) or $\beta_1 \geq 40$ and $\beta_2 = 4$ (for image blocks of size 128×128). The quality of a restored selected image block of size 64×64 (or 128×128) is expected to be very high.

Table 4. The image $N \times N$ ($N = 2^n$) compression ratio β, for different values of the parameter τ ($\tau = \beta_2 \cdot 4^{n-m}$)

τ	Compression ratio of the whole image, β_1			
	20	25	30	40
8	5.71	6.06	6.32	6.67
12	7.5	8.11	8.57	9.23
16	8.89	9.76	10.43	11.43
32	12.31	14.04	15.48	17.78
48	14.12	16.44	18.46	21.82
64	15.24	17.98	20.43	24.62
128	17.30	20.92	24.30	30.48
192	18.11	22.12	25.95	33.10
256	18.55	22.78	26.85	34.59

4. Experimental results

To corroborate the obtained theoretical results (Sections 2 and 3), some test grey-level images of size 512×512 and 256×256 were analyzed, namely: *plant.bmp* 512×512 (Figure 5; a), *survey.bmp* 512×512 (Figure 6; a) and *yard.bmp* 256×256 (Figure 7; a).

Application of the locally progressive image encoding procedure to the images 512×512 gave auspicious and fast-track results.

For instance, compression of the image *plant.bmp* at a ratio $\beta_1 = 30$ made it possible to obtain a rough image estimate (restored image; PSNR = 18.37) with still visible dislocation of objects in the plant area (Figure 5; b). Comparatively small amount of additional information (12.6 KB; compression ratio $\beta_2 = 5$) improved quality of the selected image fragment (associated with Haar spectral coefficient $Y(2,3)$) considerably – PSNR = 21.70 (Figure 5; c). One more (third) image encoding level (7.9 KB of additional information; $\beta_3 = 2$) highlighted details in the left-bottom block of the earlier selected fragment (Figure 5; d). The quality of the latter restored image block is high enough (PSNR = 23.23). The overall averaged image compression ratio $\beta = 8.96$.

Two-level processing (encoding) of the image *survey.bmp* 512×512 (Figure 6; a) can be characterized as being impressive enough – the quality of the restored image fragment (associated with the Haar spectral coefficient $Y(3,3)$) is high (PSNR = 25.08; $\beta_1 = 35$; $\beta_2 = 3$) (Figure 6; b, c). The overall image compression ratio $\beta = 9.09$.

(a)

(b)

(c)

(d)
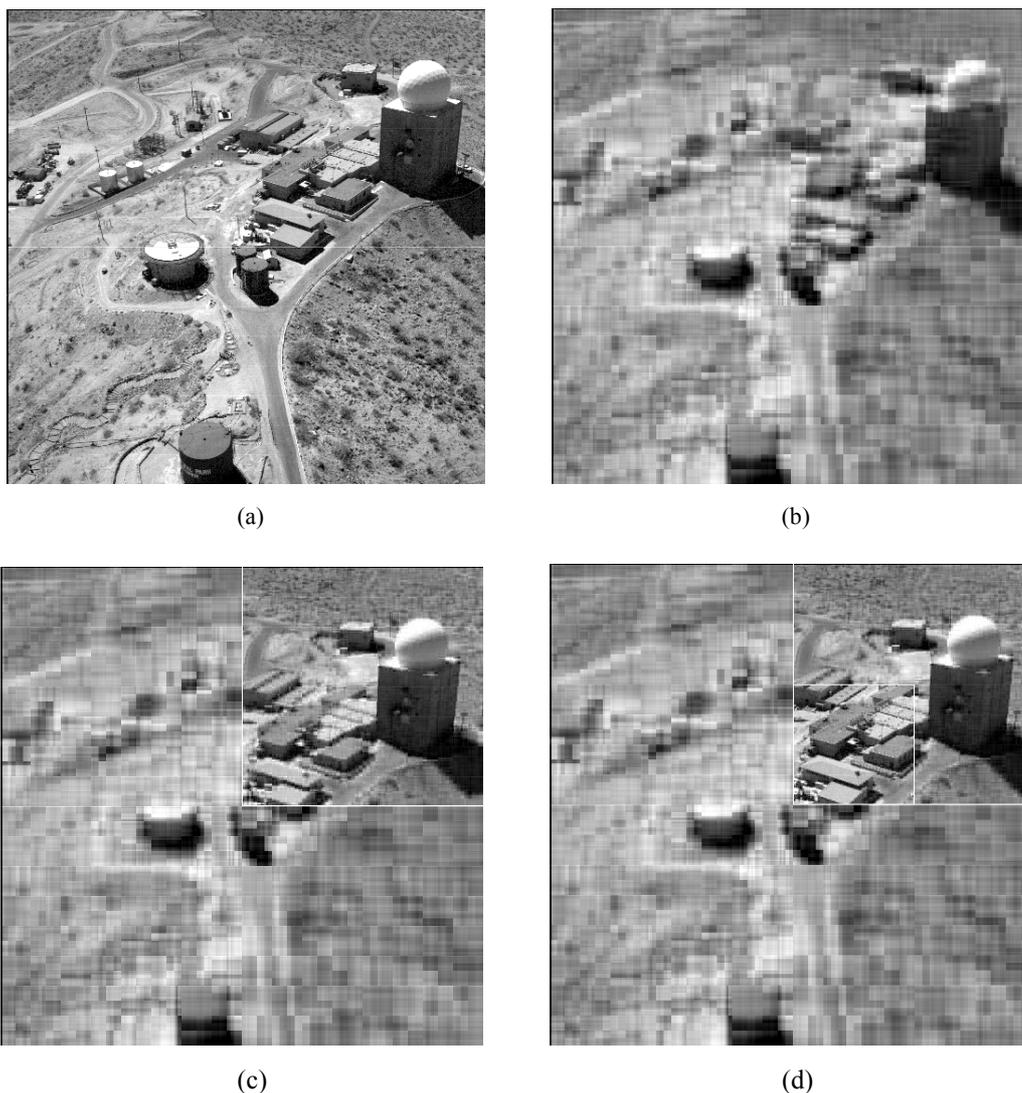
Figure 5. Locally progressive encoding of test images: (a) original image *plant.bmp* 512x512; (b) the rough estimate of the whole image ($\beta_1 = 30$); (b) the selected image fragment of size 256x256 compressed at a ratio $\beta_2 = 5$; (c) the selected image block of size 128x128 compressed at a ratio $\beta_3 = 2$ (third encoding level)

Locally progressive encoding applied to images of smaller sizes leads to similar prepossessing results. For instance, preliminary compression ($\beta_1 = 20$) of the image *yard.bmp* 256×256 (Figure 7; a) and the resulting image estimate (PSNR = 22.40) create conditions for distinguishing a moving object (a man) in the yard region (Figure 7; b). Repeated encoding of the localized region (this time, associated with the Haar spectral coefficient $Y(6,6)$; $\beta_2 = 3$) reveals some new

details (Figure 7; c; PSNR = 26.80). The averaged image compression ratio $\beta = 14.1$.

It goes without saying that the overall averaged image compression ratio β directly depends on the size of the selected image blocks (the values of β_1 and β_2 being fixed), i.e., the smaller size of the

selected image block, the higher image compression ratio β.

Finally, we here note that computer realization of the proposed locally progressive image encoding approach, based on the use of hyperbolic image filters, was done by Asta Širvelyte – Bachelor of Mathematics, Kaunas University of Technology.

| (a) | (b) | (c) |
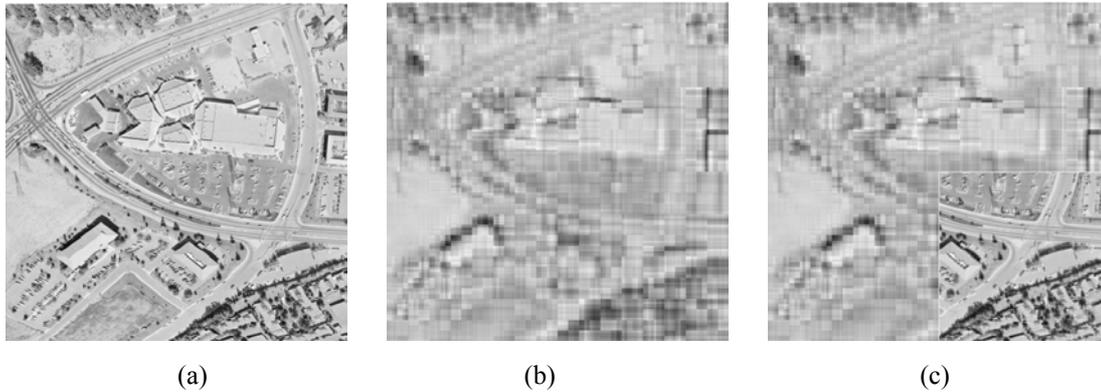
Figure 6. Locally progressive encoding of test images: (a) original image *survey.bmp* 512x512; (b) the rough estimate of the whole image ($\beta_1 = 35$); (b) the selected image fragment of size 256x256 compressed at a ratio $\beta_2 = 3$

| (a) | (b) | (c) |
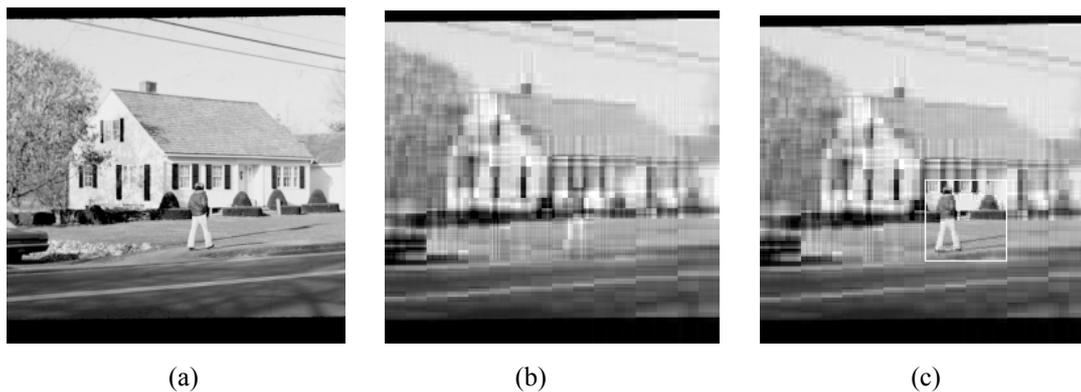
Figure 7. Locally progressive encoding of test images: (a) original image *survey.bmp* 256x256; (b) the rough estimate of the whole image ($\beta_1 = 20$); (b) the selected image fragment of size 64x64 compressed at a ratio $\beta_2 = 3$

5. Conclusion

In the paper, a new original procedure for the determination of the discrete Haar (wavelet) spectra for the selected image blocks is presented. The procedure explores specific properties of Haar wavelets, refers to the fact that the discrete HT spectrum of the whole image is known and appears to be much faster than direct evaluation of HT spectra for respective image blocks.

On the other hand, the developed procedure made it possible to develop and realize a new locally progressive (grey-level) image encoding idea. Firstly, the image under processing is compressed "heavily" using two-dimensional hyperbolic filters, secondly, the selected image blocks are highlighted by giving them more details ("soft" compression, repeated application of hyperbolic filtering). The preliminary experimental results show that the developed image encoding ap-

proach is noteworthy – the quality of restored selected image fragments (blocks) is high enough, the overall image compression ratio is tolerable.

The proposed multi-level and locally progressive image encoding procedure, undoubtedly, will find various applications in processing medical images, in implementing efficient and up-to-date digital data processing technologies (e-health, e-business, etc.).

In the future, some analysis, concerning the usage of modified hyperbolic filters is supposed. In parallels, implementation of the locally progressive image encoding approach, based on the direct use of EZW algorithm, is planned too.

References

[1]   **P. Fränti, O. Nevalainen, T. Kaukoranta**. Compression of Digital Images by Block Truncation Coding: A

survey. *The Computer Journal, Vol.*37, *No.*4, 1994, 308-332.

[2] **K. Culik II, J. Kari.** Finite state methods for compression and manipulation of images. *Proceedings of Data Compression Conference* 1995*, Snowbird, Utah*, 1995, 142-151.

[3] **K. Culik II, Vladimir Valenta.** Finite Automata Based Compression of Bi-level and Simple Color Images. *University of South Carolina, Columbia, S.C.* 29208. *USA*, 1-14.

[4] **Y. Fisher.** Fractal Image Compression – Theory and Application, *Springer-Verlag, New York*, 1994.

[5] **W. Brendt, G. de Jager**. A Review of the Fractal Image Coding Literature. *IEEE Transactions on Image Processing, Vol.*8, *No.*12, 1999, 1716-1729.

[6] **J. Valantinas, N. Morkevičius, T. Žumbakis**. Accelerating Compression Times in Block-Based Fractal Image Coding Procedures. *Proceedings of the* 20th *Eurographics UK Conference. Leicester* (*De Montfort university*, *UK*): *IEEE Computer Society Press* (*Los Alamitos*, *California*), 2002, 83-88.

[7] **J. Valantinas, R. Valantinas.** Problem-Oriented Change of Image Dimensionality. *Proceedings of the Third International Symposium on Image and Signal Processing and Analysis*, *Rome* (*Italy*), *Universita degli Studi ROMA TRE*, 2003, 228-232.

[8] **M. Polvere, M. Nappi**. Speed-Up in Fractal Image Coding: Comparison in Methods. *IEEE Transactions on Image Processing*, 9(6), 2000, 1002-1009.

[9] **C.S. Tong, M. Wong**. Adaptive approximate nearest neighbor search for fractal image compression. *IEEE Transactions on Image Processing*, 11(6), 2002, 605-615.

[10] **T. Žumbakis, J. Valantinas.** The Use of Image Smoothness Estimates in Speeding Up Fractal Image Compression. *Lecture Notes in Computer Science* 3540 (*Proceedings of the* 14*th Scandinavian Conference SCIA* 2005, *Joensuu, Finland*). ISSN 0302-9743. *Springer-Verlag Berlin Heidelberg*, 2005, 1167-1176.

[11] **N. Ahmed, K.R. Rao**. Orthogonal Transforms for Digital Signal Processing. *Springer-Verlag, Berlin, Heidelberg – New York*, 1975.

[12] **G.K. Wallace.** The JPEG Still Picture Compression Standard. *Comm. of the ACM, Vol.*34, *No.*4, 1991, 30-44.

[13] **M.W. Marcelin, M.J. Gormish, A. Bilgin, M.P. Boliek**. An Overview of JPEG-2000. *Proc. of IEEE Data Compression Conference*, 2000, 523-541.

[14] **P. Zinterhof, P.Z interhof jun.** Hyperbolic filtering of Walsh Series. *RIST++* (*University of Salzburg, Austria*), 1993.

[15] **J. Valantinas**. A new approach to hyperbolic filtering of gray-level images. *Information Technology and Control, No.*1(7), *Technologija, Kaunas*, 1998, 35–42.

[16] **J.M. Shapiro.** Embedded Image Coding Using Zerotrees of Wavelet Coefficients. *IEEE Transactions on Signal Processing, Vol.*41, *No.*12, 1993, 3445-3462.

[17] **V.R. Algazi, R.R. Estes**. Analysis based coding of image transform and subband coefficients. *Proceedings of the SPIE, Vol.*2564, 1995, 11-21.

[18] **A. Said, W.A**. **Pearlmon.** A New, Fast and Efficient Image Codec Based on Set Partitioning in Hierarchical Trees. *IEEE Trans. CSVT, Vol.*6, *No.*3, 1996, 243-250.

[19] **C.D. Creusere.** A new method of robust image compression based on the embedded zerotree wavelet algorithm. *IEEE Transactions on Image Processing, Vol.*6, *No.*10, 1997, 1436-1442.

[20] **M. Vetterli.** Wavelets, Approximation and Compression. *IEEE Signal Processing Magazine*, 2001, 59-73.